Vatalanib, a tyrosine kinase inhibitor, decreases hepatic fibrosis and sinusoidal capillarization in CCl_4-induced fibrotic mice

LING-JIAN KONG*, HAO LI*, YA-JU DU, FENG-HUA PEI, YING HU, LIAO-LIAO ZHAO and JING CHEN

Department of Gastroenterology, The Second Affiliated Hospital of Harbin Medical University, Harbin, Heilongjiang 150086, P.R. China

Received December 26, 2015; Accepted February 3, 2017

DOI: 10.3892/mmr.2017.6325

Abstract. Among the various consequence arising from lung injury, hepatic fibrosis is the most severe. Decreasing the effects of hepatic fibrosis remains one of the primary therapeutic challenges in hepatology. Dysfunction of hepatic sinusoidal endothelial cells is considered to be one of the initial events that occur in liver injury. Vascular endothelial growth factor signaling is involved in the progression of genotype changes. The aim of the present study was to determine the effect of the tyrosine kinase inhibitor, vatalanib, on hepatic fibrosis and hepatic sinusoidal capillarization in a carbon tetrachloride (CCl_4)-induced mouse model of liver fibrosis. Liver fibrosis was induced in BALB/c mice using CCl_4 by intraperitoneal injection for 6 weeks. The four experimental groups included a control, and three experimental groups involving administration of CCl_4, vatalanib and a combination of the two. Histopathological staining and measuring live hydroxyproline content evaluated the extent of liver fibrosis. The expression of α-smooth muscle actin (SMA) and cluster of differentiation (CD) 34 was detected by immunohistochemistry. Collagen type I, α-SMA, transforming growth factor (TGF)-β1 and vascular endothelial growth factor receptor (VEGFR) expression levels were measured by reverse transcription-quantitative polymerase chain reaction (RT-qPCR). The average number of fenestrae per hepatic sinusoid was determined using transmission electron microscopy. Liver fibrosis scores and hydroxyproline content were decreased in both vatalanib groups. In addition, both doses of vatalanib decreased mRNA expression levels of hepatic α-SMA, TGF-β1, collagen-1, VEGFR1, and VEGFR2. Levels of α-SMA and CD34 protein were decreased in the vatalanib group compared with the CCl_4 group. There were significant differences in the number of fenestrae per sinusoid between the groups. The present study identified that administration of vatalanib was associated with decreased liver fibrosis and hepatic sinusoidal capillarization in CCl_4-induced mouse models, and is a potential compound for counteracting liver fibrosis.

Introduction

Hepatic fibrosis is a primary consequence of liver injury that results from chronic liver diseases, including chronic viral hepatitis, alcohol and metabolic liver disease (1,2). The ultimate aim is to treat the cause of the liver disease, which may lead to the reversal of fibrosis (3,4). With emerging novel technology and refined methodologies, knowledge concerning the mechanisms underlying liver fibrosis and its pathogenesis are continuously expanding (5). However, the development of anti-fibrotic compounds represents a major therapeutic challenge (6).

Vascular endothelial growth factor (VEGF) is an important mediator of angiogenesis (7). In addition, VEGF and its receptors serve critical roles in chronic inflammation and liver fibrosis (8,9). Angiogenesis is involved in chronic inflammatory liver disease. The fact that these diseases respond poorly to conventional anti-inflammatory therapy suggests that angiogenesis may be an effective therapeutic target in reversing persistent, stable inflammation in chronic liver diseases (10). Intra-hepatic angiogenesis and sinusoidal remodeling occur in many chronic liver diseases (11). Anti-angiogenesis treatment may be a therapeutic approach in liver fibrosis and portal hypertension (11). It has been previously reported that anti-angiogenesis drugs, including sorafenib, sunitinib, and Endostar, which are used in the treatment of carcinoma, inhibit hepatocellular carcinoma and liver fibrosis (12-15).

Vatalanib, also known as PTK/ZK, is an orally active, small molecule tyrosine kinase inhibitor that is effective against all VEGF receptors (16,17). It has been demonstrated that the combination of vatalanib and intravenous doxorubicin administration has encouraging activity in treating advanced hepatocellular carcinoma (HCC) patients (18). In China, the

Correspondence to: Dr Jing Chen, Department of Gastroenterology, The Second Hospital of Harbin Medical University, 246 Xuefu Road, Nan-gang, Harbin, Heilongjiang 150086, P.R. China
E-mail: mchenjing7@medmail.com.cn

*Contributed equally

Abbreviations: TGF-β, transforming growth factor-β; HSC, hepatic stellate cell; α-SMA, α-smooth muscle actin; VEGF, vascular endothelial growth factor; VEGFR, vascular endothelial growth factor receptor; ALT, alanine aminotransferase; AST, aspartate aminotransferase; TBIL, total bilirubin; TEM, transmission electron microscopy

Key words: carbon tetrachloride, hepatic fibrosis, vatalanib, hepatic sinusoidal cell capillarization, vascular endothelial growth factor

majority of HCC patients have co-existing hepatitis B and liver cirrhosis (19). A previous study indicated that vatalanib had anti-fibrotic effects in experimental liver fibrosis *in vivo* (20). However, the underlying mechanism by which this occurs remains unclear. The aim of the current study was to determine the anti-fibrogenic effects of vatalanib in terms of pathological alterations of the liver and hepatic sinusoidal endothelial cell (SEC) phenotypes in CCl_4-induced fibrotic mice.

Materials and methods

Mouse model of CCl_4-induced liver fibrosis. Vatalanib was purchased from LC Laboratories (Woburn, MA, USA; cat. no. V-8303), and dissolved in 100 mg/ml distilled water. A total of 32 male BALB/c mice weighing 18-20 g were obtained from Beijing Vital River Laboratory Animal Technology (Beijing, China). The Animal Care and Use Committee of Harbin Medical University approved all protocols and procedures (Harbin, China). Animals were housed in an air-conditioned room at 23-25˚C with a 12-h dark/light cycle for one week prior to the initiation of experiments. All animals received appropriate care during the study with unlimited access to food and water.

Liver fibrosis was induced in mice by intraperitoneal injection of CCl_4 (40% CCl_4 in olive oil, 0.2 ml/100 g body weight, twice weekly) for 6 weeks as previously reported (21). A total of four groups were studied: Group 1, normal control mice; group 2, CCl_4 alone; group 3, CCl_4 + vatalanib (50 mg/kg/d by gavage for 6 weeks, vatalanib was administered simultaneously with a CCl_4 injection for 6 weeks); and group 4, CCl_4 + vatalanib (50 mg/kg/d by gavage for 4 weeks, CCl_4 alone was administered to mice for 2 weeks, following which vatalanib was administered to mice simultaneously with CCl_4 injection for another 4 weeks). In the previous study, vatalanib (50 and 100 mg/kg/d) was well tolerated by the mice, and had no significant effects on body weight (22). Therefore, 50 mg/kg/d was used in the present study. Previous studies identified that CCl_4-induced hepatic fibrosis is present after 2 weeks (20). Group 1 received olive oil intraperitoneally at the same dose and conditions as the CCl_4-treated mice.

Mice were euthanized (via 2% pentobarbital i.p. at 0.3 ml/100 g body weight) and liver samples were immediately snap-frozen in liquid nitrogen and stored at -80˚C until further use. An additional section was embedded in paraffin and sliced into 4-5 μm sections.

Histological examination. Sections were stained with hematoxylin and eosin and Sirius Red (Solarbio Life Sciences, Beijing, China) for histopathological analysis and liver fibrosis evaluation. Each sample was independently assessed and scored by two pathologists, blinded to the study protocol, according to a fibrosis score system (16). Liver fibrosis was divided into seven stages: 0, no fibrosis; 1, short fibrous tissue in central venule (C); 2, fibrous between central venule and central venule (C-C) septa appearance; 3, C-C fibrous septa incompletely developed; 4, C-C septa completely connected (pseudo-lobule); 5, C-P (portal tract) bridging fibrosis, nodular appearance ≤50%; and 6, nodular appearance >50%.

Hepatic hydroxyproline analyses. Hepatic hydroxyproline was measured using a hydroxyproline detection kit (Jiancheng Institute of Biotechnology, Nanjing, China) according to the manufacturer's protocol. The hydroxyproline content is expressed as mg/g wet liver.

Transmission electron microscopy (TEM). Samples were processed for TEM as described previously (23). Fresh specimens were fixed in 3% glutaraldehyde (Beijing Brilliance Biochemical Company, Beijing, China), washed with PBS, and fixed in 1% osmic acid for 60 min. The samples were dehydrated through an alcohol series, embedded in EPON 812 epoxy resin (Hede Biotechnology Co., Ltd., Beijing, China), and then cut into 50 nm sections with an ultrathin microtome. Following staining with uranyl acetate and lead citrate for 30 min, the sections were examined using a transmission electron microscope (cat. no. H-7650; Hitachi, Ltd., Tokyo, Japan). A total of 10 hepatic sinusoids with a diameter of 2-3 μm were randomly selected from each group and subgroup, and the mean number of fenestrae per hepatic sinusoid was determined. Each sample was independently assessed and scored by two pathologists, both blinded to the study protocol.

Biochemical analyses. Blood was collected from the inferior vena cava. Serum alanine aminotransferase (ALT), aspartate aminotransferase (AST), total bilirubin (TBIL) and albumin were assayed using an automatic biochemical analyzer (cat. no. 7600; Hitachi, Tokyo, Japan).

Immunohistochemistry staining for α-SMA and CD34. CD34 is a marker of newly-formed blood vessels. The vascular density in portal and peri-portal areas was assessed by determining the number of CD34-labeled vessel sections (24). Liver tissue samples were fixed in 10% formalin for 1 week at room temperature, sliced into 4-6 mm pieces, dehydrated in ethanol and embedded in paraffin wax. α-SMA and CD34 were detected in paraffin-embedded liver sections (4-5 μm thick) using the following specific primary antibodies: α-SMA (cat. no. A2547; Sigma-Aldrich; Merck Millipore, Darmstadt, Germany) and CD34 (cat no. ab81289; Abcam, Cambridge, MA, USA) and an avidin-biotin complex immunoperoxidase method (15). Following antigen retrieval by immersion in EDTA (1 mmol/l, pH 8.0) and boiling for 15 min, sections were pre-blocked with normal goat serum for 10 min, and incubated for 2 h at room temperature with specific antibodies (α-SMA, dilution 1:200; CD34, dilution, 1:200). PBS was used in place of the primary antibodies for the negative controls. Following rinsing, the biotinylated secondary antibody (goat anti-rabbit IgG, cat no. ZDR-5307, goat anti-mouse IgG, cat. no. ZDR-5306, OriGene Technologies, Inc., Beijing, China), avidin-biotin complex and horseradish peroxidase (Strept ABComplex; Dako; Agilent Technologies, Inc., Santa Clara, CA, USA) were applied. Finally, the sections were washed with PBS, developed with diaminobenzidine tetrahydrochloride substrate (Strept ABComplex; Dako; Agilent Technologies, Inc.) for 3 min, and counterstained with hematoxylin.

Computer-assisted semi-quantitative analysis was used to evaluate the areas of positive α-SMA and CD34 staining using Image-ProPlus software (version 4.5; Media Cybernetics, Inc., Rockville, MD, USA). The data for the α-SMA and CD34 staining are expressed as the mean percentage of the positively stained area relative to the total tissue section area (17).

Table I. Primers for reverse transcription-quantitative polymerase chain reaction analysis.

Gene	Direction	Primer sequence (5'-3')	Accession number
GAPDH (mouse)	F	GCACAGTCAAGGCCGAGAAT	XM_001476707.3
	R	GCCTTCTCCATGGTGGTGAA	
Col I a1 (mouse)	F	TTCACCTACAGCACGCTTGTG	NM_007742.3
	R	GATGACTGTCTTGCCCCAAGTT	
α-SMA (mouse)	F	TCAGCGCCTCCAGTTCCT	NM_007392.2
	R	AAAAAAAACCACGAGTAACAAATCAA	
TGF-β1 (mouse)	F	CCCGAACCCCCATTGCTGTCC	NM_011577.1
	R	AGGCGTATCAGTGGGGGTCAG	
VEGFR1 (mouse)	F	CCACCTCTCTATCCGCTGG	NM_010228.3
	R	ACCAATGTGCTAACCGTCTTATT	
VEGFR2 (mouse)	F	CAAACCTCAATGTGTCTCTTTGC	NM_010612.2
	R	AGAGTAAAGCCTATCTCGCTGT	

Col I a1, type I collagen; α-SMA, α-smooth muscle actin; TGF-β1, transforming growth factor-β1; VEGFR, vascular endothelial growth factor receptor; F, forward; R, reverse; CCl_4, carbon tetrachloride.

Table II. Effects of vatalanib on CCl_4-induced liver fibrosis.

	Liver fibrosis score							
Group	0	1	2	3	4	5	6	Mean ± standard deviation
1 (n=7)	7	0	0	0	0	0	0	0
2 (n=8)	0	0	0	0	2	5	1	4.88±0.64
3 (n=8)	0	0	4	3	1	0	0	2.6±0.74[a]
4 (n=8)	0	0	3	3	1	1	0	3.0±1.07[a]

CCl_4, carbon tetrachloride. Group 1, normal control; group 2, CCl_4 model; group 3, CCl_4 + vatalanib (6 weeks, 50 mg/kg); and group 4, CCl_4 + vatalanib (4 weeks, 50 mg/kg). [a]P<0.01 vs. CCl_4 group.

Measurement of mRNA levels of collagen I, α-SMA, TGF-β1, VEGFR1 and VEGFR2 by RT-qPCR. Total RNA was extracted from liver tissues and HSC-T6 cells using a TRIzol® Reagent kit (Invitrogen; Thermo Fisher Scientific, Inc., Waltham, MA, USA) according to the manufacturer's protocol. The quality of total RNA was verified by ultraviolet absorbance spectrophotometry at 260 and 280 nm. cDNA was reversed transcribed using the High-Capacity cDNA Reverse Transcription kit (Applied Biosystems; Thermo Fisher Scientific, Inc.), according to the manufacturer's protocol. The thermocycling parameters were as follows: 25˚C for 10 min, 37˚C for 150 min, 85˚C for 5 sec, and 4˚C for 5 min for one cycle, before chilling on ice. cDNA was stored at -20˚C until further required. Collagen I, α-SMA, TGF-β1, VEGFR1 and VEGFR2 mRNA levels were quantified using the primers presented in Tables I and II. GAPDH, a housekeeping gene, was used as an internal control primer for target genes. All primers were obtained from Invitrogen; Thermo Fisher Scientific, Inc. The expression of mRNA was measured by SYBR Green Real-Time PCR using an ABI 7500 instrument (Applied Biosystems; Thermo Fisher Scientific, Inc.). PCR was performed in 20 μl buffer that contained 2 μg cDNA, 1 μl each primer and 10 μl SYBR Green PCR Master Mix (Applied Biosystems; Thermo Fisher Scientific, Inc.). Comparative quantitation threshold (Cq) calculations were all relative to the control group. The expression of mRNA relative to the control was derived using the equation $2^{-\Delta\Delta Cq}$ (25).

Statistical analysis. The results are expressed as the mean ± standard deviation. Statistical analysis was performed by analysis of one way analysis of variance and unpaired Student's t-test as appropriate. Non-parametric data were analyzed by the Mann-Whitney U-test. P<0.05 was considered to indicate a statistically significant difference. Statistical analyses were performed using SPSS (version 17.0; SPSS Inc., Chicago, IL, USA). Data are presented as the mean ± standard deviation.

Results

Vatalanib inhibits liver fibrosis in CCl_4-induced mice. There were no collagen fibers along the central vein in control group 1 (Fig. 1A). In group 2, collagenous fibers extended from the central vein and the portal area to the hepatic lobules with pseudo-lobule formation (Fig. 1B). With administration of

Table III. Effects of vatalanib on biochemical markers in CCl_4-treated mice.

	Group 1 (n=7)	Group 2 (n=8)	Group 3 (n=8)	Group 4 (n=8)
Hydroxyproline (mg/g liver)	0.1±0.04	92.0±4.6	54.2±5.4[a]	49.8±6.9[a]
ALT (IU/ml)	38.4±5.9	149.5±19.4	98.8±14.6[a]	109.2±10.4[a]
AST (IU/ml)	41.0±8.3	235.5±16.8	149.0±14.8[a]	153.9±19.0[a]
TBIL (mg/dl)	1.0±0.1	1.9±0.2	1.8±0.3	1.8±0.2
Albumin (g/l)	34.8±1.5	26.2±1.9	28.6±1.6	29.2±1.8

ALT, alanine aminotransferase; AST, aspartate aminotransferase; TBIL, total bilirubin; CCl_4, carbon tetrachloride. Group 1, normal control; group 2, CCl_4 model; group 3, CCl_4 + vatalanib (6 weeks, 50 mg/kg); and group 4, CCl_4 + vatalanib (4 weeks, 50 mg/kg). Data are expressed as the mean ± standard deviation. [a]P<0.01 (vatalanib group vs. CCl_4 group).

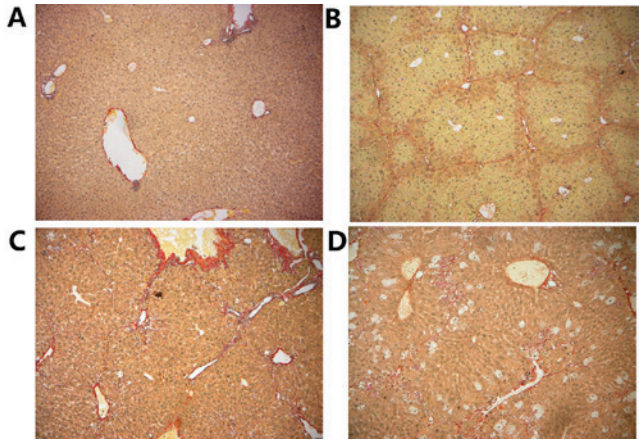

Figure 1. Vatalanib attenuates the extent of liver fibrosis in CCl_4-stimulated mice. Representative photomicrographs of Sirius Red staining in groups (A) 1, control; (B) 2, CCl_4 model; (C) 3, CCl_4 + vatalanib (6 weeks, 50 mg/kg) and (D) 4, CCl_4 + vatalanib (4 weeks, 50 mg/kg). Magnification, x100. CCl_4, carbon tetrachloride.

vatalanib (50 mg/kg/d, for 4 or 6 weeks) in groups 3 (Fig. 1C) and 4 (Fig. 1D), collagenous fibers were decreased compared with group 2. The fibrosis scores following vatalanib administration in groups 3 and 4 were significantly reduced when compared with those in group 2 (P<0.05; Table II). In addition, vatalanib reduced hydroxyproline concentrations in liver tissue, reflecting decreased total hepatic collagen content (P<0.01; Table III).

Vatalanib reduces liver inflammation. Serum ALT and AST levels were significantly decreased following vatalanib treatment (P<0.01), whereas no significant alterations in serum TBIL and albumin levels were observed (P>0.05; Table III).

Vatalanib inhibits α-SMA and CD34 protein levels. Levels of α-SMA, a typical marker of activated HSCs, were assessed by immunohistochemistry to evaluate the effect of vatalanib on HSC activation during hepatic fibrosis. There was no positive staining in control group 1 (Fig. 2A). CCl_4 alone led to considerable increases in the amount of α-SMA positive cells, which were distributed throughout the fibrotic septa (Fig. 2B). Computer-assisted semi-quantitative analysis revealed that vatalanib-treated groups (groups 3 and 4) presented significantly decreased α-SMA-positive areas compared with group 2 (P<0.05; Fig. 2C-E). These results demonstrated that vatalanib decreased the number of activated HSCs.

There was little positive CD34 staining in the control group 1 (Fig. 2F). Following six weeks of CCl_4 induction, this led to significant increases in the number of CD34 positive cells, while groups 3 and 4 presented significantly decreased CD34 positive areas compared with group 2 (P<0.05; Fig. 2G-J).

Ultrastructural changes in fibrotic mice after vatalanib treatment. There were significantly increased fenestrae per SEC in group 1 (Fig. 3A) compared with group 2 (Fig. 3B; P<0.01; Table IV). In group 2, the microvilli of hepatocytes in the perisinusoidal space and the intra-lobular bile ducts (cholangioles) disappeared (Fig. 3C), and the junctions between hepatocytes were destroyed (Fig. 3D). In group 3, the number of fenestrae was significantly increased compared with group 2 (P<0.01; Fig. 3E; Table IV), and cholangioles appeared morphologically healthy (Fig. 3F). Group 4 additionally had an increased number of fenestrae compared with group 2 (Fig. 3G; Table IV), and presented with cell junctions similar to normal control mice (Fig. 3H). There were no significant differences in the numbers of fenestrae between groups 3 and 4 (P>0.05). The extent of hepatocyte necrosis and inflammation was less so in groups 3 and 4 compared with group 2.

Vatalanib was associated with decreased collagen I, α-SMA, TGF-β1, VEGFR1 and VEGFR2 mRNA levels. mRNA expression levels of collagen I, α-SMA, TGF-β1, VEGFR1 and VEGFR2 were increased in group 2 compared with group 1 (P<0.01; Fig. 4). mRNA levels were reduced in groups 3 and 4 compared with group 2 (P<0.01).

Discussion

Intrahepatic hypoxia may occur during the liver inflammatory and fibrotic processes that characterize several chronic liver diseases (26). As a consequence, intrahepatic vascular angiogenesis and sinusoidal remodeling may occur in these chronic liver diseases (8,26). In previous years, numerous studies have examined the expression of various anti-angiogenic molecules in chronic liver disease (26). Among these molecules, VEGF and its receptors are of the most important, and have been fully studied in terms of their roles in liver inflammation

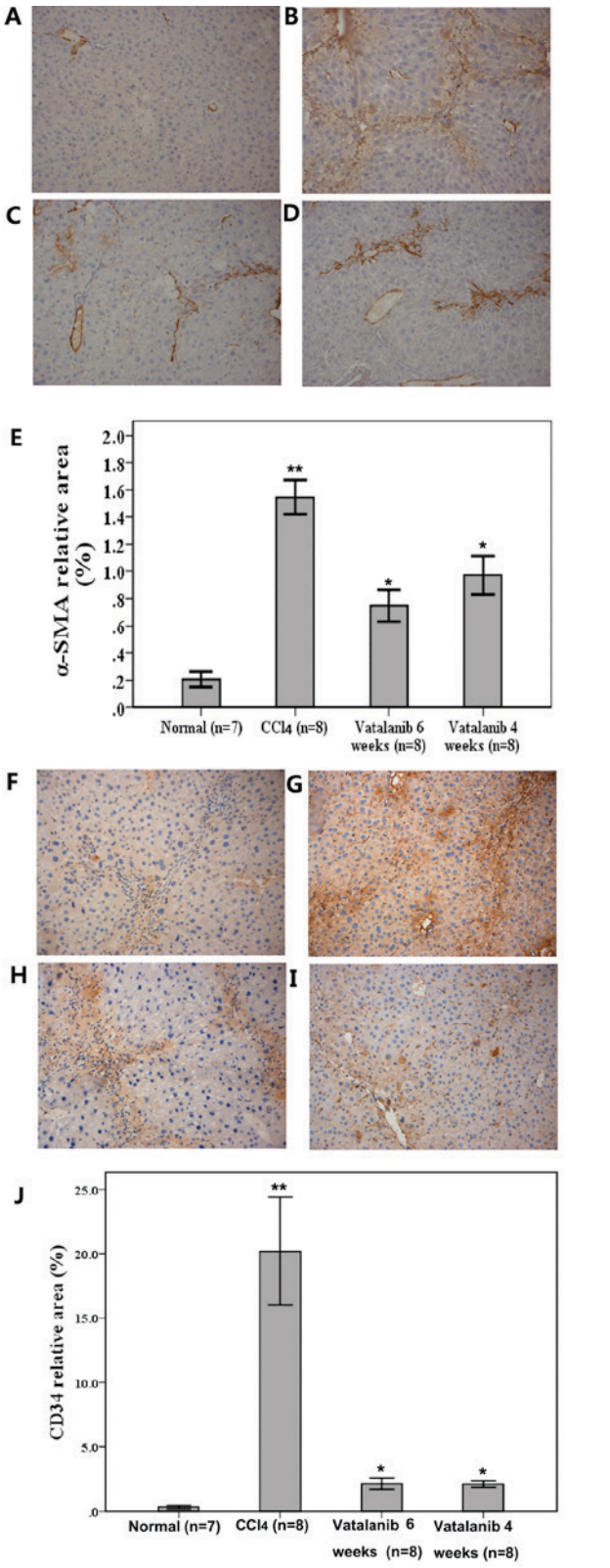

Figure 2. Vatalanib suppresses α-SMA and CD34 expression in CCl_4-induced fibrotic mouse livers. Representative photomicrographs of immunohistochemistry staining of α-SMA expression in the following groups: (A) 1, normal control; (B) 2, CCl_4 model; (C) 3, CCl_4 + vatalanib (6 weeks, 50 mg/kg) and (D) 4, CCl_4 + vatalanib (4 weeks, 50 mg/kg). (E) Semi-quantitative analysis of the immunohistochemical staining. (F-J) Representative photomicrographs of immunohistochemical staining of CD34 expression in groups (F) 1, (G) 2, (H) 3 and (I) 4. (J) Semi-quantitative analysis of the immunohistochemical staining. Magnification, x100. α-SMA, α-smooth muscle actin; CCl_4, carbon tetrachloride; CD34, cluster of differentiation 34. Data are presented as the mean ± standard deviation. *P<0.05 vatalanib vs. CCl_4 group. **P<0.05 CCl_4 vs. normal group.

Table IV. Quantitation of hepatic sinusoidal endothelial cell fenestrae.

Group	Number of fenestrae
1 (n=7)	7.43±0.98
2 (n=8)	2.38±0.91
3 (n=8)	4.75±0.71[a]
4 (n=8)	3.88±0.64[a]

[a]P<0.01 vs. group 2.

and fibrosis (26,27). Anti-VEGF treatment may represent a potential therapeutic approach in liver fibrosis and portal hypertension (10,28).

Vatalanib has been previously identified to specifically block VEGF-induced phosphorylation of VEGFR-1, -2 and -3 and inhibit endothelial cell proliferation, differentiation and tumor angiogenesis (29). It is considered safe for patients in previous cancer studies (30,31). The most common grade 3 and 4 non-hematological toxicities are mucositis and alopecia (17,18,32).

In addition, Liu *et al* (20) investigated the role of vatalanib in CCl_4-induced mice. They identified that vatalanib decreases liver fibrosis in a CCl_4-induced liver fibrosis model. This result is consistent with current findings. However, they examined the effect of vatalanib in liver fibrosis and HSCs, not SECs. The present study examined the effects of vatalanib on the number of hepatic SEC fenestrae, and levels of VEGFR in liver tissues. The results suggested that vatalanib may exert its effects via the VEGF signaling pathway. The present results reinforced the concept that angiogenesis has a major role in liver fibrogenesis (8,10,33,34).

The underlying molecular mechanism by which vatalanib decreases liver injury remains unknown. It has been demonstrated that, in primary HSCs, vatalanib decreases the levels of α-SMA, collagen, tissue inhibitor of metalloproteinase-1, and reduces cell proliferation, migration and actin filament formation. This effect was associated with inhibition of VEGF, PDGF and TGF-β1 signaling and their downstream target, protein kinase B (35). In the current study, vatalanib was identified to inhibit TGF-β1, VEGFR1 and VEGFR2.

Dysfunction of SECs is likely to be one of the initial events in liver injury (36). Defenestration and capillarization of the sinusoidal endothelium may be major contributors to hepatic failure in hepatic cirrhosis (36). Two studies from 2010 suggested that intrahepatic angiogenesis and sinusoidal remodeling may be involved in sinusoidal resistance, fibrosis and portal hypertension (11,37). In the present study, vatalanib altered the SEC phenotype, leading to decreased sinusoidal capillarization. Microvilli disappearance, inflammation, hepatocyte necrosis and bile duct alterations were decreased in all vatalanib-treated groups. These results indicated that anti-angiogenic agents may inhibit SECs, and that they may be involved in sinusoidal capillarization and hepatocyte damage. SECs may be potential target cells in the inhibition of this process. Furthermore, it is understood that paracrine signaling between SECs and HSCs regulates fibrogenesis, angiogenesis and portal hypertension

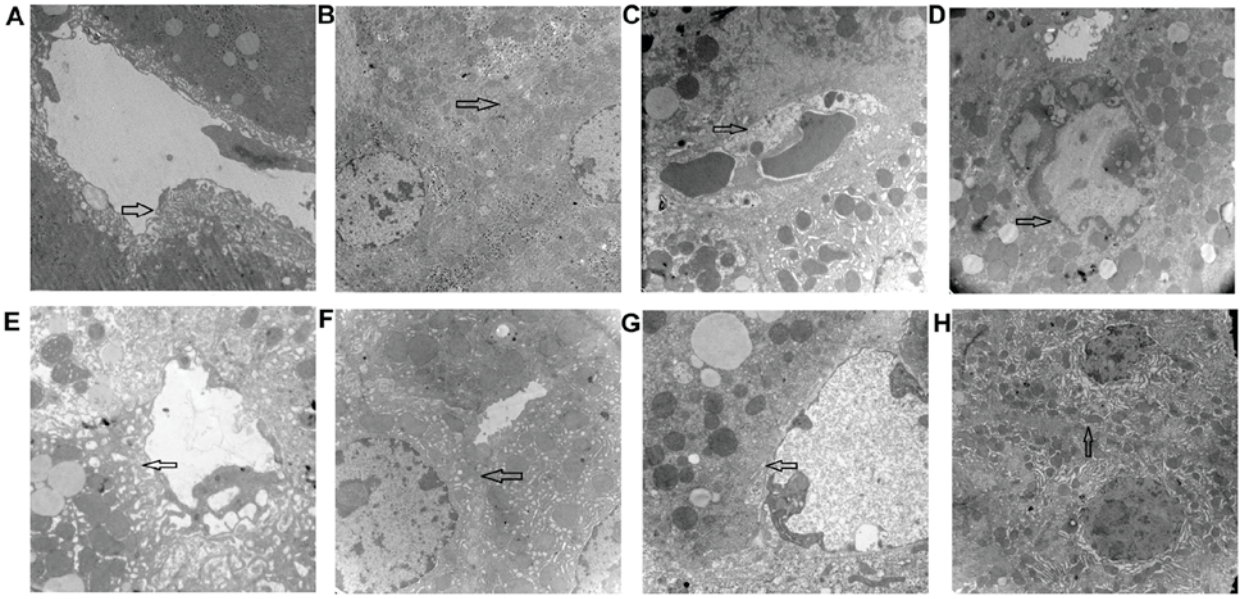

Figure 3. CCl_4-stimulates SEC capillarization, cholangiole extension and decreased hepatocyte microvilli. Vatalanib attenuated SEC capillarization and decreased the damage in cholangioles, microvilli and cell junctions between hepatocytes. Representative images representing different fields of views of the four groups. Group 1 exhibiting (A) normal SECs, fenestrae and (B) cell junctions between hepatocytes. Group 2 was in a fibrotic state and exhibited (C) disappearance of SEC fenestrae and the appearance of a basement membrane, and (D) disappearance of cell junctions with cholangiole extension, and karyopyknosis in hepatocytes. Group 3, treated with vatalanib (6 weeks, 50 mg/kg) presented with (E) fenestrae of SECs similar to those of normal control mice and (F) cell junctions between hepatocytes similar to normal control mice. Group 4 treated with vatalanib (4 weeks, 50 mg/kg) demonstrated (G) fenestrae of SECs similar to normal control mice and (H) cell junctions between hepatocytes similar to normal control mice. Magnification, x12,000. CCl_4, carbon tetrachloride; SEC, sinusoidal endothelial cell.

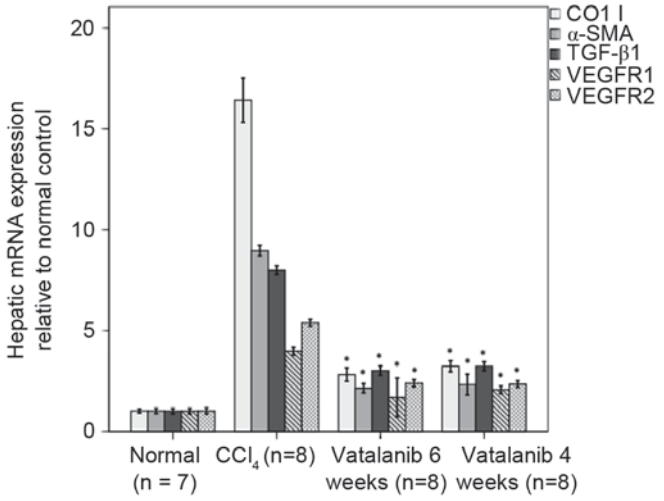

Figure 4. Vatalanib inhibits mRNA expression levels of collagen I, α-SMA, TGF-β1, VEGFR1 and VEGFR2 in fibrotic mice. mRNA expression of collagen I, α-SMA, TGF-β1, VEGFR1 and VEGFR2 were determined by reverse transcription-quantitative polymerase chain reaction in the livers treated with or without vatalanib. Data were normalized to the internal control (GAPDH) and are expressed as the mean ± standard deviation. $^*P<0.01$ vs. CCl_4 group. α-SMA, α-smooth muscle actin; TGF-β1, transforming growth factor-β1; VEGFR, vascular endothelial growth factor receptor; CCl_4, carbon tetrachloride.

in chronic liver disease (8,9,14,38). In the present study, the underlying mechanism of vatalanib on SECs was not addressed. Therefore, the nature of the interactions between SECs and HSCs in chronic liver disease following vatalanib treatment requires further investigation.

In conclusion, vatalanib treatment was associated with decreased hepatic sinusoidal capillarization, hepatocyte damage and liver fibrosis in CCl_4-induced fibrotic mice. Vatalanib may represent a potential therapeutic agent for counteracting hepatic fibrosis.

Acknowledgements

The present study was supported by the Natural Science Foundation of Heilongjiang Province of China (grant no. H2015099).

References

1. Friedman SL: Cellular networks in hepatic fibrosis. Digestion 59: 368-371, 1998.
2. Friedman SL: Hepatic fibrosis-overview. Toxicology 254: 120-129, 2008.
3. Ghiassi-Nejad Z and Friedman SL: Advances in antifibrotic therapy. Expert Rev Gastroenterol Hepatol 2: 803-816, 2008.
4. Jiao J, Friedman SL and Aloman C: Hepatic fibrosis. Curr Opin Gastroenterol 25: 223-229, 2009.
5. Friedman SL: Liver fibrosis: From mechanisms to treatment. Gastroenterol Clin Biol 31: 812-814, 2007.
6. Friedman SL and Bansal MB: Reversal of hepatic fibrosis-fact or fantasy? Hepatology 43 (2 Suppl 1): S82-S88, 2006.
7. Ferrara N and Davis-Smyth T: The biology of vascular endothelial growth factor. Endocr Rev 18: 4-25, 1997.
8. Coulon S, Heindryckx F, Geerts A, Van Steenkiste C, Colle I and Van Vlierberghe H: Angiogenesis in chronic liver disease and its complications. Liver Int 31: 146-162, 2011.
9. Fernández M, Semela D, Bruix J, Colle I, Pinzani M and Bosch J: Angiogenesis in liver disease. J Hepatol 50: 604-620, 2009.
10. Lai WK and Adams DH: Angiogenesis and chronic inflammation; The potential for novel therapeutic approaches in chronic liver disease. J Hepatol 42: 7-11, 2005.
11. Thabut D and Shah V: Intrahepatic angiogenesis and sinusoidal remodeling in chronic liver disease: New targets for the treatment of portal hypertension? J Hepatol 53: 976-980, 2010.

12. Mejias M, Garcia-Pras E, Tiani C, Miquel R, Bosch J and Fernandez M: Beneficial effects of sorafenib on splanchnic, intrahepatic and portocollateral circulations in portal hypertensive and cirrhotic rats. Hepatology 49: 1245-1256, 2009.
13. Majumder S, Piguet AC, Dufour JF and Chatterjee S: Study of the cellular mechanism of Sunitinib mediated inactivation of activated hepatic stellate cells and its implications in angiogenesis. Eur J Pharmacol 705: 86-95, 2013.
14. Thabut D, Routray C, Lomberk G, Shergill U, Glaser K, Huebert R, Patel L, Masyuk T, Blechacz B, Vercnocke A, *et al*: Complementary vascular and matrix regulatory pathways underlie the beneficial mechanism of action of sorafenib in liver fibrosis. Hepatology 54: 573-585, 2011.
15. Chen J, Liu DG, Yang G, Kong LJ, Du YJ, Wang HY, Li FD, Pei FH, Song JT, Fan YJ, *et al*: Endostar, a novel human recombinant endostatin, attenuates liver fibrosis in CCl4-induced mice. Exp Biol Med (Maywood) 239: 998-1006, 2014.
16. Jones SF, Spigel DR, Yardley DA, Thompson DF and Burris HA III: A phase I trial of vatalanib (PTK/ZK) in combination with bevacizumab in patients with refractory and/or advanced malignancies. Clin Adv Hematol Oncol 9: 845-852, 2011.
17. Thomas AL, Morgan B, Drevs J, Unger C, Wiedenmann B, Vanhoefer U, Laurent D, Dugan M and Steward WP: Vascular endothelial growth factor receptor tyrosine kinase inhibitors: PTK787/ZK 222584. Semin Oncol 30 (3 Suppl 6): S32-S38, 2003.
18. Yau T, Chan P, Pang R, Ng K, Fan ST and Poon RT: Phase 1-2 trial of PTK787/ZK222584 combined with intravenous doxorubicin for treatment of patients with advanced hepatocellular carcinoma: Implication for antiangiogenic approach to hepatocellular carcinoma. Cancer 116: 5022-5029, 2010.
19. Yang Y, Jin L, He YL, Wang K, Ma XH, Wang J, Yan Z, Feng YL, Li YQ, Chen TY, *et al*: Hepatitis B virus infection in clustering of infection in families with unfavorable prognoses in northwest China. J Med Virol 85: 1893-1899, 2013.
20. Liu Y, Lui EL, Friedman SL, Li L, Ye T, Chen Y, Poon RT, Wo J, Kok TW and Fan ST: PTK787/ZK22258 attenuates stellate cell activation and hepatic fibrosis in vivo by inhibiting VEGF signaling. Lab Invest 89: 209-221, 2009.
21. Wang H, Zhang Y, Wang T, You H and Jia J: N-methyl-4-isoleucine cyclosporine attenuates CCl-induced liver fibrosis in rats by interacting with cyclophilin B and D. J Gastroenterol Hepatol 26: 558-567, 2011.
22. Liu Y, Poon RT, Li Q, Kok TW, Lau C and Fan ST: Both antiangiogenesis- and angiogenesis-independent effects are responsible for hepatocellular carcinoma growth arrest by tyrosine kinase inhibitor PTK787/ZK222584. Cancer Res 65: 3691-3699, 2005.
23. Xu H, Shi BM, Lu XF, Liang F, Jin X, Wu TH and Xu J: Vascular endothelial growth factor attenuates hepatic sinusoidal capillarization in thioacetamide-induced cirrhotic rats. World J Gastroenterol 14: 2349-2357, 2008.
24. Elpek GÖ, Unal B and Bozova S: H-ras oncogene expression and angiogenesis in experimental liver cirrhosis. Gastroenterol Res Pract 2013: 868916, 2013.
25. Livak KJ and Schmittgen TD: Analysis of relative gene expression data using real-time quantitative PCR and the 2(-Delta Delta C(T)) method. Methods 25: 402-408, 2001.
26. Medina J, Arroyo AG, Sánchez-Madrid F and Moreno-Otero R: Angiogenesis in chronic inflammatory liver disease. Hepatology 39: 1185-1195, 2004.
27. Calderone V, Gallego J, Fernandez-Miranda G, Garcia-Pras E, Maillo C, Berzigotti A, Mejias M, Bava FA, Angulo-Urarte A, Graupera M, *et al*: Sequential functions of CPEB1 and CPEB4 regulate pathologic expression of vascular endothelial growth factor and angiogenesis in chronic liver disease. Gastroenterology 150: 982-997.e30, 2016.
28. Fernandez M, Vizzutti F, Garcia-Pagan JC, Rodes J and Bosch J: Anti-VEGF receptor-2 monoclonal antibody prevents portal-systemic collateral vessel formation in portal hypertensive mice. Gastroenterology 126: 886-894, 2004.
29. Schomber T, Zumsteg A, Strittmatter K, Crnic I, Antoniadis H, Littlewood-Evans A, Wood J and Christofori G: Differential effects of the vascular endothelial growth factor receptor inhibitor PTK787/ZK222584 on tumor angiogenesis and tumor lymphangiogenesis. Mol Cancer Ther 8: 55-63, 2009.
30. Kircher SM, Nimeiri HS and Benson AB III: Targeting angiogenesis in colorectal cancer: Tyrosine kinase inhibitors. Cancer J 22: 182-189, 2016.
31. Dragovich T, Laheru D, Dayyani F, Bolejack V, Smith L, Seng J, Burris H, Rosen P, Hidalgo M, Ritch P, *et al*: Phase II trial of vatalanib in patients with advanced or metastatic pancreatic adenocarcinoma after first-line gemcitabine therapy (PCRT O4-001). Cancer Chemother Pharmacol 74: 379-387, 2014.
32. Langenberg MH, Witteveen PO, Lankheet NA, Roodhart JM, Rosing H, van den Heuvel IJ, Beijnen JH and Voest EE: Phase 1 study of combination treatment with PTK 787/ZK 222584 and cetuximab for patients with advanced solid tumors: Safety, pharmacokinetics, pharmacodynamics analysis. Neoplasia 12: 206-213, 2010.
33. Vanheule E, Geerts AM, Van Huysse J, Schelfhout D, Praet M, Van Vlierberghe H, De Vos M and Colle I: An intravital microscopic study of the hepatic microcirculation in cirrhotic mice models: Relationship between fibrosis and angiogenesis. Int J Exp Pathol 89: 419-432, 2008.
34. Ferrara N and Kerbel RS: Angiogenesis as a therapeutic target. Nature 438: 967-974, 2005.
35. Liu Y, Wen XM, Lui EL, Friedman SL, Cui W, Ho NP, Li L, Ye T, Fan ST and Zhang H: Therapeutic targeting of the PDGF and TGF-beta-signaling pathways in hepatic stellate cells by PTK787/ZK22258. Lab Invest 89: 1152-1160, 2009.
36. Braet F and Wisse E: Structural and functional aspects of liver sinusoidal endothelial cell fenestrae: A review. Comp Hepatol 1: 1, 2002.
37. Huebert RC, Jagavelu K, Liebl AF, Huang BQ, Splinter PL, LaRusso NF, Urrutia RA and Shah VH: Immortalized liver endothelial cells: A cell culture model for studies of motility and angiogenesis. Lab Invest 90: 1770-1781, 2010.
38. Friedman SL: Preface. Hepatic fibrosis: Pathogenesis, diagnosis and emerging therapies. Clin Liver Dis 12: xiii-xiv, 2008.